

TS-SSC 91-240  
12/9/91  
J. Strait

## Shell Axial Stress Change with Excitation in DCA311 and DCA312

The long 50 mm magnets built at Fermilab are instrumented with strain gauges on the cold mass shell as shown in Figure 1. Strain gauge packages SG1 - SG7 consist of azimuthal-axial pairs at 7 axial locations. Their primary purpose is to measure the axial shell stress under excitation as a function of the distance from the end of the magnet. At the position of SG5 there is also an array of gauges to measure the azimuthal strain as a function of angle from the yoke parting plane. The data from the axial array is the subject of this note.

I have analysed the data from one strain gauge run from each of DCA311 and DCA312: DCA311.CA015 was taken during a ramp to quench at 3.5 K and is the highest current run taken; DCA312.CA004 was taken during a ramp to quench at 4.35 K and was the highest current run at the time I did the analysis. The data are displayed, along with the results of various calculations, in Tables I and II. Table section (a) gives the strains as read from the CRYOLOG files. The columns are labeled by the Keithley channel numbers and by an "a" or "l" (for azimuthal and axial strain gauges) followed by the distance, in inches, from the return (non-lead) end of the yoke. The distances on Figure 1 are measured from the end plate to shell weld. Section (b) shows the change in strain relative to  $I=0$ , with the axial and azimuthal strains separated. Next in section (d) are the stress changes in the axial ( $z$ ) and azimuthal ( $a$ ) directions, calculated with the Poisson effect resolved using the parameters in section (c). Here the columns are labeled by the axial position in millimeters and the stresses are in MPa. Next the axial stress is multiplied by the cross sectional area of the shell to yield the axial force, displayed in section (e). Finally in section (f) the axial force is divided by the calculated axial Lorentz force[1] to facilitate comparison between runs to different peak currents.

Figures 2 and 3 show the axial and azimuthal strains as a function of current squared for DCA311; the same is shown for DCA312 in Figures 6 and 7. The data are reasonably linear in  $I^{**2}$  as expected. The axial strains are generally extensive and the azimuthal strains are generally compressive and smaller than the axial strains. Figures 4 and 8 show the axial and azimuthal strains and stresses as a function of  $z$  at the highest current of the runs for DCA311 and DCA312 respectively. The correction for the Poisson effect has little effect on the axial stress calculation, but has a more significant effect on the azimuthal stresses. With modest fluctuations, the azimuthal stresses are on the average approximately zero. (The azimuthal location of the axial gauge array was chosen, based on short magnet data[2], to be where azimuthal stress changes with excitation are small.)

Figures 5 and 9 show the axial shell force (assuming that the axial stress is azimuthally symmetric) as a function of  $z$ . In both magnets the force reaches a maximum of about 60% of the calculated Lorentz force a little over

one meter from the end of the yoke and then drops somewhat towards the magnet center. The Lorentz force is balanced by the stretching of the shell and of the coil. Some of the force is transmitted to the shell "directly" through the end plate. This is known from the bullet gauges to be a small fraction of the total force. A much larger fraction is transmitted to the shell via coil-collar-yoke-shell friction. Assuming a frictional force independent of  $z$  then the force on the shell should rise linearly with  $z$  until the coil and shell are fully locked together. Farther into the magnet the coil and shell stretch together, sharing the load with equal strain. Taken at face value, the fact that the shell carries at most 60% of the Lorentz force implies that the coil axial spring constant is about 2/3 of that of the shell. I have not tried to make a serious calculation of the coil spring constant, but this ratio seems surprisingly high to me.

Between the measurements at 1300 and 2000 mm is one of the cryostat support posts, and another post is between the 2000 mm point and the 7250 mm point (near the magnet center). In DCA311 there is a significant force decrease between 2000 mm and the center, and in DCA312 there is a more modest decrease across the first post. The measured axial strains imply an overall stretching of the cold mass of about 0.4-0.5 mm per end. If the cold mass does not slide perfectly at a post, then the post will deflect and then the Lorentz force will be shared by the post as well. I do not know the stiffness of the posts, so I do not know if it is plausible for a post to carry as large a fraction of the Lorentz force as is implied by the shell gauge data.

At a qualitative level, the axial shell gauge data indicate that the magnet is behaving in the expected manner: the tight yoke-collar fit causes the axial component of the Lorentz force to be transmitted to the shell over a length of about 1 meter from the end. The behaviors of the first two magnets are very similar to each other and both are similar to the 40 mm magnets.

#### FOOTNOTES

- [1] The axial Lorentz force is taken to be the rate of change of stored energy with magnet length:  $dE/dz = 105 \text{ kJ/m} = 105 \text{ kN}$  at 6500 A from Ramesh Gupta's article on the Magnetic Design, section 2.3.1 of the "Yellow Book." The Lorentz force is taken to be proportional to current squared.
- [2] J. Strait, et al., Mechanical behavior of Fermilab-built 1.5 m model SSC collider dipoles, submitted to the 12th International Conference on Magnet Technology (MT12), Leningrad, USSR, 1-5 July, 1991.

DISTRIBUTION: W.Boroski, R.Bossert, J.Carson, S.Delchamps, A.Devred, J.DiMarco, W.Koska, J.Kuzminski, M.J.Lamm, P.O.Mazur, T.Nicol, D.Orris, E.G.Pewitt, M.Wake

dca311 shell ca015  
Table I

DCA311.CA015 25-NOV-1991

strain gauge loop to 7700A after 3.85K quench tests, at 2nd testing cycle, 3.5 K

(a)

K001	K123	K099	K100	K101	K102	K103	K104	K106	K107	K108	K109	K111	K112	K114	K115
Ibefore	Iafter	I(1.9)	a(1.9)	I(7.8)	a(7.8)	I(18)	a(18)	I(31)	a(31)	I(51)	a(51)	I(79)	a(79)	I(285)	a(285)
52.7	52.6	-12.5	8.2	-28.8	3.5	-7.6	34.0	10.1	9.4	-11.1	31.7	-46.0	1.4	-7.1	-14.0
2187.8	2187.8	-13.6	7.6	-28.3	1.9	-2.8	33.5	17.1	9.4	-1.4	30.6	-39.0	-0.7	-3.9	-15.6
3180.4	3180.5	-14.1	6.0	-27.7	0.3	3.1	34.0	24.6	8.9	7.2	27.9	-31.5	-3.4	0.9	-17.7
4470.9	4470.8	-14.6	3.9	-26.7	-2.4	8.5	32.9	36.4	7.3	21.6	22.0	-18.7	-7.7	9.0	-22.0
4967.7	4967.6	-13.6	3.3	-25.6	-3.4	10.6	34.0	42.2	7.2	28.0	19.9	-12.2	-9.3	12.8	-23.6
5861.0	5861.1	-12.5	2.8	-24.0	-4.5	14.9	35.1	53.5	7.3	41.4	16.2	0.6	-12.5	19.7	-27.9
6258.1	6258.2	-12.5	2.3	-24.5	-5.6	16.5	36.2	58.3	6.8	46.3	13.5	6.6	-15.1	23.5	-30.0
6655.2	6655.3	-11.4	1.2	-24.0	-6.6	17.6	37.2	62.6	5.7	52.7	11.9	14.1	-15.1	26.7	-32.7
7052.2	7052.1	-10.9	1.2	-22.9	-7.2	18.6	37.7	68.0	6.7	58.6	9.7	20.5	-16.7	31.0	-34.8
7350.4	7350.2	-11.5	0.1	-23.5	-8.8	19.6	39.3	73.3	6.7	63.9	8.1	26.4	-17.8	34.2	-35.4
7648.5	7647.7	-11.5	0.7	-22.4	-7.7	20.8	39.9	77.1	5.7	68.3	7.0	31.2	-20.0	37.4	-37.0

(b)

I**2	$\Delta I$	$\Delta \mu e(z)$						$\Delta \mu e(a)$								
		I(1.9)	I(7.8)	I(18)	I(31)	I(51)	I(79)	I(285)	I**2	a(1.9)	a(7.8)	a(18)	a(31)	a(51)	a(79)	a(285)
0.0	-0.1	0.0	0.0	0.0	0.0	0.0	0.0	0.0	0.0	0.0	0.0	0.0	0.0	0.0	0.0	0.0
4.8	0.0	-1.1	0.5	4.8	7.0	9.7	7.0	3.2	4.8	-0.6	-1.6	-0.5	0.0	-1.1	-2.1	-1.6
10.1	0.1	-1.6	1.1	10.7	14.5	18.3	14.5	8.0	10.1	-2.2	-3.2	0.0	-0.5	-3.8	-4.8	-3.7
20.0	-0.1	-2.1	2.1	16.1	26.3	32.7	27.3	16.1	20.0	-4.3	-5.9	-1.1	-2.1	-9.7	-9.1	-8.0
24.7	-0.1	-1.1	3.2	18.2	32.1	39.1	33.8	19.9	24.7	-4.9	-6.9	0.0	-2.2	-11.8	-10.7	-9.6
34.4	0.1	0.0	4.8	22.5	43.4	52.5	46.6	26.8	34.4	-5.4	-8.0	1.1	-2.1	-15.5	-13.9	-13.9
39.2	0.1	0.0	4.3	24.1	48.2	57.4	52.6	30.6	39.2	-5.9	-9.1	2.2	-2.6	-18.2	-16.5	-16.0
44.3	0.1	1.1	4.8	25.2	52.5	63.8	60.1	33.8	44.3	-7.0	-10.1	3.2	-3.7	-19.8	-16.5	-18.7
49.7	-0.1	1.6	5.9	26.2	57.9	69.7	66.5	38.1	49.7	-7.0	-10.7	3.7	-2.7	-22.0	-18.1	-20.8
54.0	-0.2	1.0	5.3	27.2	63.2	75.0	72.4	41.3	54.0	-8.1	-12.3	5.3	-2.7	-23.6	-19.2	-21.4
58.5	-0.8	1.0	6.4	28.4	67.0	79.4	77.2	44.5	58.5	-7.5	-11.2	5.9	-3.7	-24.7	-21.4	-23.0

(c)

2.1E+05	Modulus (MPa)
0.3	Poisson ratio
5210	x-sect area of shell (mm**2)
105000	F(Lorentz) at operating current (N)
6.5	Operating current (kA)

Table I  
dca311 shell ca015

(d)

I**2	z(mm)	$\Delta\text{stress}(z)$ (MPa)							$\Delta\text{stress}(a)$ (MPa)						
		47	197	447	797	1297	1997	7247	47	197	447	797	1297	1997	7247
0.0		0.00	0.00	0.00	0.00	0.00	0.00	0.00	0.00	0.00	0.00	0.00	0.00	0.00	0.00
4.8		-0.29	0.00	1.06	1.59	2.13	1.45	0.62	-0.21	-0.33	0.21	0.48	0.41	0.00	-0.15
10.1		-0.51	0.03	2.43	3.26	3.90	2.97	1.57	-0.61	-0.65	0.73	0.88	0.38	-0.10	-0.30
20.0		-0.77	0.08	3.59	5.84	6.78	5.59	3.12	-1.12	-1.20	0.85	1.32	0.03	-0.21	-0.72
24.7		-0.58	0.26	4.14	7.15	8.09	6.96	3.87	-1.19	-1.35	1.24	1.69	-0.02	-0.13	-0.83
34.4		-0.37	0.55	5.19	9.73	10.88	9.65	5.15	-1.23	-1.49	1.79	2.48	0.06	0.02	-1.33
39.2		-0.40	0.36	5.63	10.79	11.81	10.84	5.87	-1.34	-1.78	2.15	2.70	-0.22	-0.16	-1.55
44.3		-0.23	0.40	5.95	11.69	13.16	12.55	6.41	-1.52	-1.97	2.45	2.74	-0.15	0.35	-1.95
49.7		-0.11	0.61	6.21	12.99	14.35	13.89	7.25	-1.48	-2.03	2.63	3.34	-0.25	0.42	-2.13
54.0		-0.33	0.37	6.55	14.19	15.45	15.16	7.93	-1.77	-2.44	3.06	3.70	-0.25	0.57	-2.05
58.5		-0.28	0.69	6.86	14.99	16.38	16.10	8.55	-1.64	-2.11	3.28	3.73	-0.20	0.40	-2.20

(e)

I**2	z(mm)	$\Delta F(z)$ (N)						
		47	197	447	797	1297	1997	7247
0.0		0	0	0	0	0	0	0
4.8		-1517	24	5511	8296	11105	7549	3224
10.1		-2678	166	12681	17007	20337	15478	8166
20.0		-4018	391	18690	30422	35305	29119	16236
24.7		-3046	1339	21569	37261	42143	36253	20171
34.4		-1920	2844	27057	50688	56709	50285	26820
39.2		-2098	1861	29344	56199	61556	56472	30576
44.3		-1185	2098	31003	60904	68572	65360	33409
49.7		-593	3188	32366	67659	74782	72376	37758
54.0		-1695	1908	34120	73940	80494	78977	41337
58.5		-1481	3603	35755	78088	85318	83884	44561

(f)

I**2	z(mm)	$\Delta F(z)/F(\text{Lorentz})$						
		47	197	447	797	1297	1997	7247
0.0		0	0	0	0	0	0	0
4.8		-0.13	0.00	0.46	0.70	0.93	0.63	0.27
10.1		-0.11	0.01	0.50	0.68	0.81	0.62	0.32
20.0		-0.08	0.01	0.38	0.61	0.71	0.59	0.33
24.7		-0.05	0.02	0.35	0.61	0.69	0.59	0.33
34.4		-0.02	0.03	0.32	0.59	0.66	0.59	0.31
39.2		-0.02	0.02	0.30	0.58	0.63	0.58	0.31
44.3		-0.01	0.02	0.28	0.55	0.62	0.59	0.30
49.7		0.00	0.03	0.26	0.55	0.61	0.59	0.31
54.0		-0.01	0.01	0.25	0.55	0.60	0.59	0.31
58.5		-0.01	0.02	0.25	0.54	0.59	0.58	0.31

Table II

dca312 shell ca004

DCA312.ca004 05-DEC-1991

Strain gauge ramp to quench; 16A/sec below 6500A, 4A/sec above

Axial array at theta = 28o

K001 Ibefore	K117 Iafter	K087 I(1.9)	K088 a(1.9)	K089 I(7.8)	K090 a(7.8)	K091 I(18)	K092 a(18)	K094 I(31)	K095 a(31)	K096 I(51)	K097 a(51)	K099 I(79)	K100 a(79)	K102 I(285)	K103 a(285)
39.0	39.1	10.7	6.5	6.8	7.7	-43.9	6.1	2.9	2.7	5.1	13.0	3.4	8.4	-5.5	-5.1
1577.8	1577.9	11.2	6.4	8.0	7.2	-41.8	5.5	6.0	2.7	8.9	13.0	5.5	6.7	-2.3	-6.2
2222.9	2222.8	10.1	4.8	8.5	6.1	-39.6	4.5	7.7	1.1	11.6	10.3	8.3	6.2	1.0	-7.3
2719.2	2719.1	9.6	3.3	9.0	4.0	-40.1	1.3	9.2	-1.0	14.7	8.8	9.8	3.0	3.1	-8.8
3141.5	3141.4	9.1	2.7	9.5	4.0	-36.9	1.8	11.9	-2.1	17.4	7.1	13.6	2.5	5.8	-10.5
3513.8	3513.7	9.6	2.2	10.1	2.9	-35.3	0.2	15.2	-1.0	22.3	7.7	16.2	0.8	9.5	-11.0
3861.0	3861.0	9.6	1.6	11.1	3.5	-32.1	0.7	18.4	-2.1	25.5	6.6	20.0	0.3	12.2	-12.0
4159.2	4159.1	9.0	0.0	11.1	1.8	-31.0	-0.9	20.0	-3.7	28.2	4.5	22.6	-0.8	14.8	-13.1
4456.1	4456.0	9.1	-0.5	11.7	1.9	-28.8	-1.9	23.2	-4.2	32.5	4.0	25.9	-1.8	18.6	-12.6
4952.7	4952.7	8.5	-1.6	13.3	0.8	-25.7	-3.5	28.0	-5.9	38.9	1.3	31.2	-5.5	23.9	-15.3
5449.2	5449.2	8.0	-3.7	13.9	-0.8	-22.4	-5.2	32.8	-8.0	45.3	-1.5	37.6	-6.6	29.2	-18.0
5846.1	5846.2	8.5	-3.7	15.4	-1.4	-19.2	-6.2	37.7	-8.5	51.7	-2.5	42.5	-8.8	34.6	-18.5
6441.5	6441.4	7.9	-5.3	18.1	-1.9	-14.4	-8.9	44.1	-9.6	59.8	-5.1	50.0	-10.8	43.7	-19.5

I**2	$\Delta I$	$\Delta \mu e(z)$						$\Delta \mu e(a)$								
		I(1.9)	I(7.8)	I(18)	I(31)	I(51)	I(79)	I(285)	I**2	a(1.9)	a(7.8)	a(18)	a(31)	a(51)	a(79)	a(285)
0.0	0.1	0.0	0.0	0.0	0.0	0.0	0.0	0.0	0.0	0.0	0.0	0.0	0.0	0.0	0.0	0.0
2.5	0.1	0.5	1.2	2.1	3.1	3.8	2.1	3.2	2.5	-0.1	-0.5	-0.6	0.0	0.0	-1.7	-1.1
4.9	-0.1	-0.6	1.7	4.3	4.8	6.5	4.9	6.5	4.9	-1.7	-1.6	-1.6	-1.6	-2.7	-2.2	-2.2
7.4	-0.1	-1.1	2.2	3.8	6.3	9.6	6.4	8.6	7.4	-3.2	-3.7	-4.8	-3.7	-4.2	-5.4	-3.7
9.9	-0.1	-1.6	2.7	7.0	9.0	12.3	10.2	11.3	9.9	-3.8	-3.7	-4.3	-4.8	-5.9	-5.9	-5.4
12.3	-0.1	-1.1	3.3	8.6	12.3	17.2	12.8	15.0	12.3	-4.3	-4.8	-5.9	-3.7	-5.3	-7.6	-5.9
14.9	0.0	-1.1	4.3	11.8	15.5	20.4	16.6	17.7	14.9	-4.9	-4.2	-5.4	-4.8	-6.4	-8.1	-6.9
17.3	-0.1	-1.7	4.3	12.9	17.1	23.1	19.2	20.3	17.3	-6.5	-5.9	-7.0	-6.4	-8.5	-9.2	-8.0
19.9	-0.1	-1.6	4.9	15.1	20.3	27.4	22.5	24.1	19.9	-7.0	-5.8	-8.0	-6.9	-9.0	-10.2	-7.5
24.5	0.0	-2.2	6.5	18.2	25.1	33.8	27.8	29.4	24.5	-8.1	-6.9	-9.6	-8.6	-11.7	-13.9	-10.2
29.7	0.0	-2.7	7.1	21.5	29.9	40.2	34.2	34.7	29.7	-10.2	-8.5	-11.3	-10.7	-14.5	-15.0	-12.9
34.2	0.1	-2.2	8.6	24.7	34.8	46.6	39.1	40.1	34.2	-10.2	-9.1	-12.3	-11.2	-15.5	-17.2	-13.4
41.5	-0.1	-2.8	11.3	29.5	41.2	54.7	46.6	49.2	41.5	-11.8	-9.6	-15.0	-12.3	-18.1	-19.2	-14.4

2.1E+05	Modulus (MPa)
0.3	Poisson ratio
5210	x-sect area of shell (mm**2)
105000	F(Lorentz) at operating current (N)
6.5	Operating current (kA)

(d)

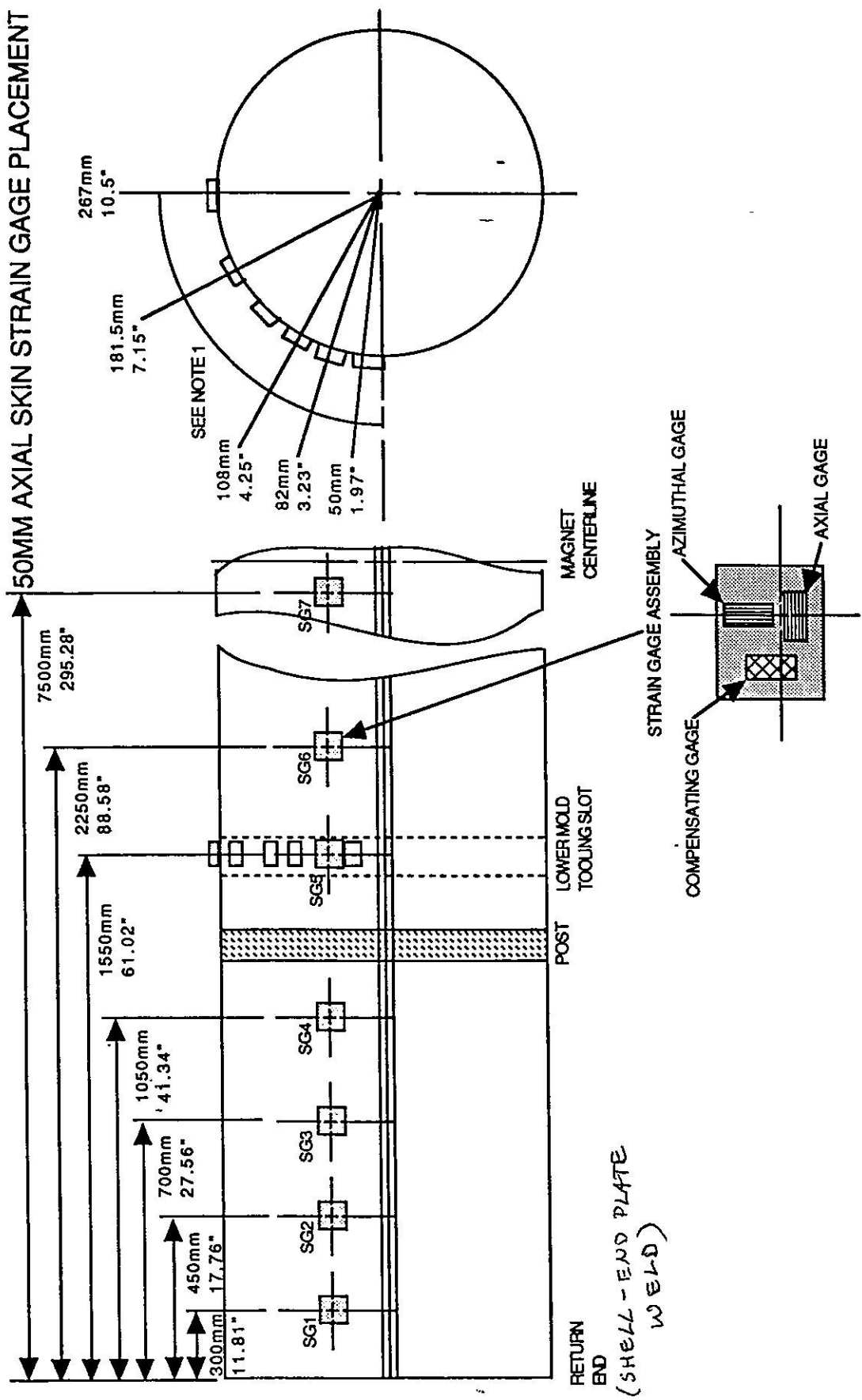
I**2	z(mm)	$\Delta\text{stress}(z)$ (MPa)							$\Delta\text{stress}(a)$ (MPa)						
		47	197	447	797	1297	1997	7247	47	197	447	797	1297	1997	7247
0.0		0.00	0.00	0.00	0.00	0.00	0.00	0.00	0.00	0.00	0.00	0.00	0.00	0.00	0.00
2.5		0.11	0.24	0.44	0.71	0.86	0.36	0.65	0.01	-0.03	0.01	0.21	0.26	-0.24	-0.03
4.9		-0.25	0.28	0.87	0.98	1.29	0.96	1.33	-0.43	-0.25	-0.07	-0.04	-0.17	-0.17	-0.06
7.4		-0.47	0.25	0.54	1.18	1.90	1.09	1.70	-0.80	-0.69	-0.83	-0.41	-0.30	-0.79	-0.25
9.9		-0.62	0.36	1.30	1.72	2.40	1.92	2.20	-0.97	-0.66	-0.50	-0.48	-0.50	-0.65	-0.46
12.3		-0.54	0.42	1.55	2.55	3.55	2.39	3.01	-1.05	-0.87	-0.76	0.00	-0.03	-0.86	-0.32
14.9		-0.58	0.69	2.32	3.20	4.20	3.22	3.56	-1.19	-0.66	-0.42	-0.03	-0.06	-0.71	-0.36
17.3		-0.83	0.58	2.46	3.45	4.67	3.74	4.07	-1.59	-1.05	-0.71	-0.29	-0.36	-0.78	-0.43
19.9		-0.84	0.72	2.89	4.15	5.62	4.42	4.97	-1.70	-0.98	-0.79	-0.18	-0.18	-0.78	-0.06
24.5		-1.05	1.01	3.48	5.12	6.89	5.38	5.99	-1.99	-1.13	-0.94	-0.24	-0.35	-1.26	-0.31
29.7		-1.31	1.04	4.12	6.07	8.15	6.76	7.01	-2.50	-1.45	-1.10	-0.39	-0.56	-1.08	-0.57
34.2		-1.20	1.34	4.78	7.15	9.54	7.72	8.21	-2.47	-1.48	-1.11	-0.17	-0.35	-1.24	-0.31
41.5		-1.44	1.92	5.69	8.53	11.21	9.29	10.21	-2.88	-1.41	-1.40	0.01	-0.38	-1.19	0.08

(e)

I**2	z(mm)	$\Delta F(z)$ (N)						
		47	197	447	797	1297	1997	7247
0.0		0	0	0	0	0	0	0
2.5		557	1244	2275	3674	4504	1884	3401
4.9		-1315	1446	4527	5120	6743	5025	6921
7.4		-2441	1292	2797	6151	9884	5665	8877
9.9		-3247	1884	6767	8960	12479	9991	11472
12.3		-2832	2204	8094	13262	18500	12468	15679
14.9		-3046	3603	12065	16663	21901	16793	18524
17.3		-4326	2998	12799	17990	24354	19484	21214
19.9		-4385	3745	15051	21605	29273	23039	25895
24.5		-5487	5250	18156	26689	35898	28005	31216
29.7		-6826	5392	21463	31631	42487	35198	36538
34.2		-6234	6957	24900	37261	49716	40223	42760
41.5		-7514	9979	29628	44454	58391	48401	53189

(f)

I**2	z(mm)	$\Delta F(z)/F(\text{Lorentz})$						
		47	197	447	797	1297	1997	7247
0.0		0	0	0	0	0	0	0
2.5		0.09	0.20	0.37	0.59	0.73	0.30	0.55
4.9		-0.11	0.12	0.37	0.42	0.55	0.41	0.56
7.4		-0.13	0.07	0.15	0.33	0.54	0.31	0.48
9.9		-0.13	0.08	0.28	0.37	0.51	0.41	0.47
12.3		-0.09	0.07	0.26	0.43	0.60	0.41	0.51
14.9		-0.08	0.10	0.33	0.45	0.59	0.45	0.50
17.3		-0.10	0.07	0.30	0.42	0.57	0.45	0.49
19.9		-0.09	0.08	0.31	0.44	0.59	0.47	0.52
24.5		-0.09	0.09	0.30	0.44	0.59	0.46	0.51
29.7		-0.09	0.07	0.29	0.43	0.58	0.48	0.50
34.2		-0.07	0.08	0.29	0.44	0.59	0.47	0.50
41.5		-0.07	0.10	0.29	0.43	0.57	0.47	0.52



- NOTES:
1. DIMENSIONS ARE RADIAL, FROM CENTER OF ALIGNMENT KEY TO CENTER OF STRAIN GAGE.
  2. GAGE ASSEMBLIES 1,4,6 AND 7 ARE TO INCLUDE COMPENSATING GAGES.
  3. FOUR COMPENSATING BLOCKS TO BE WELDED.
  4. INDIVIDUAL GAGES IN A GAGE ASSEMBLY SHOULD BE WIRED TOGETHER SERIALLY AT THE CONNECTOR.
  5. GAGE WIRES MUST EXIT CRYOSTAT AT LEAD END OF MAGNET.

MIKE GORDON  
7/13/91

Figure 1

### Axial Shell Strain Change (DCA311.CA015)

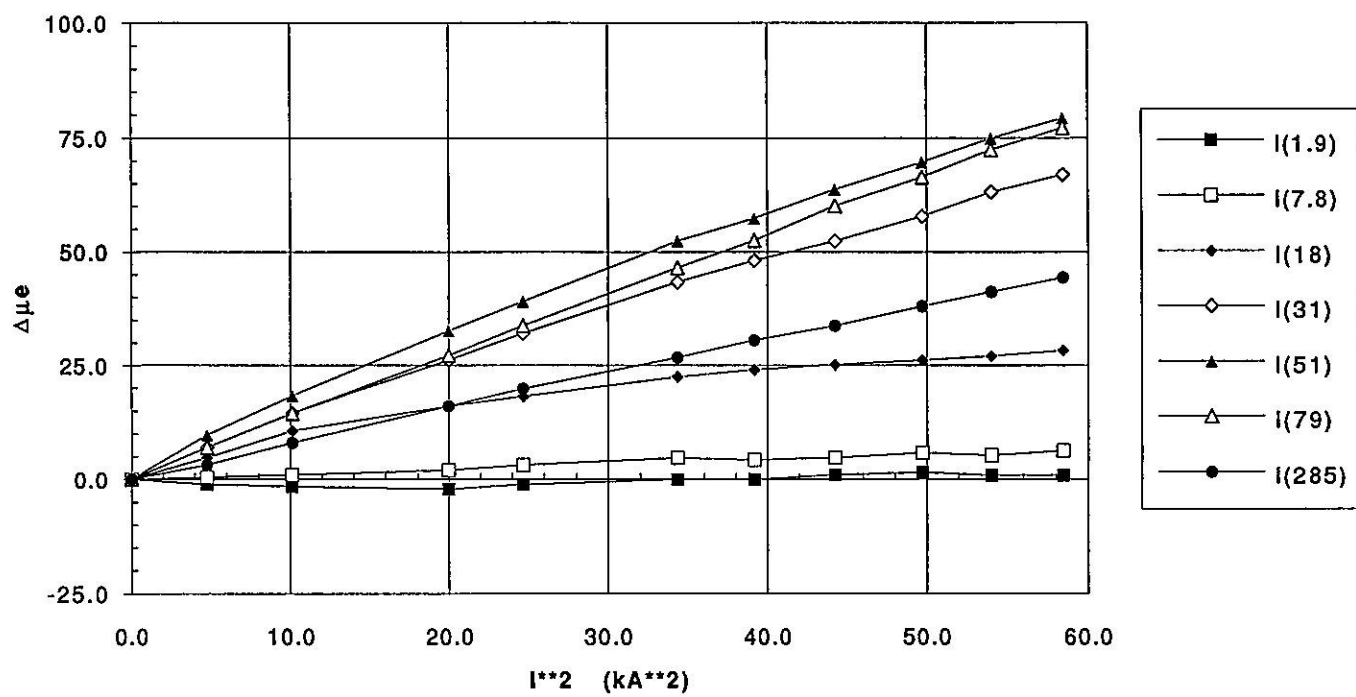


Figure 2

### Azimuthal Shell Strain Change (DCA311.CA015)

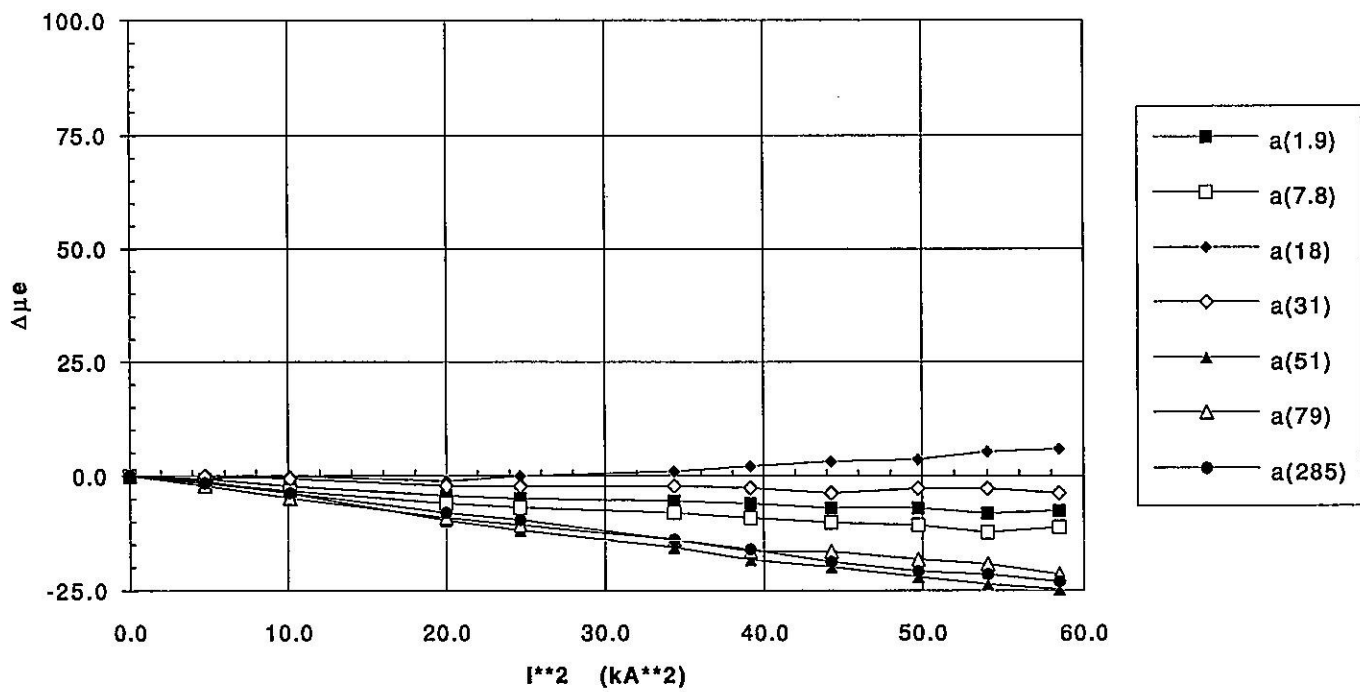


Figure 3

### DCA311 Shell Strain Gauges: Change to I=7660 A

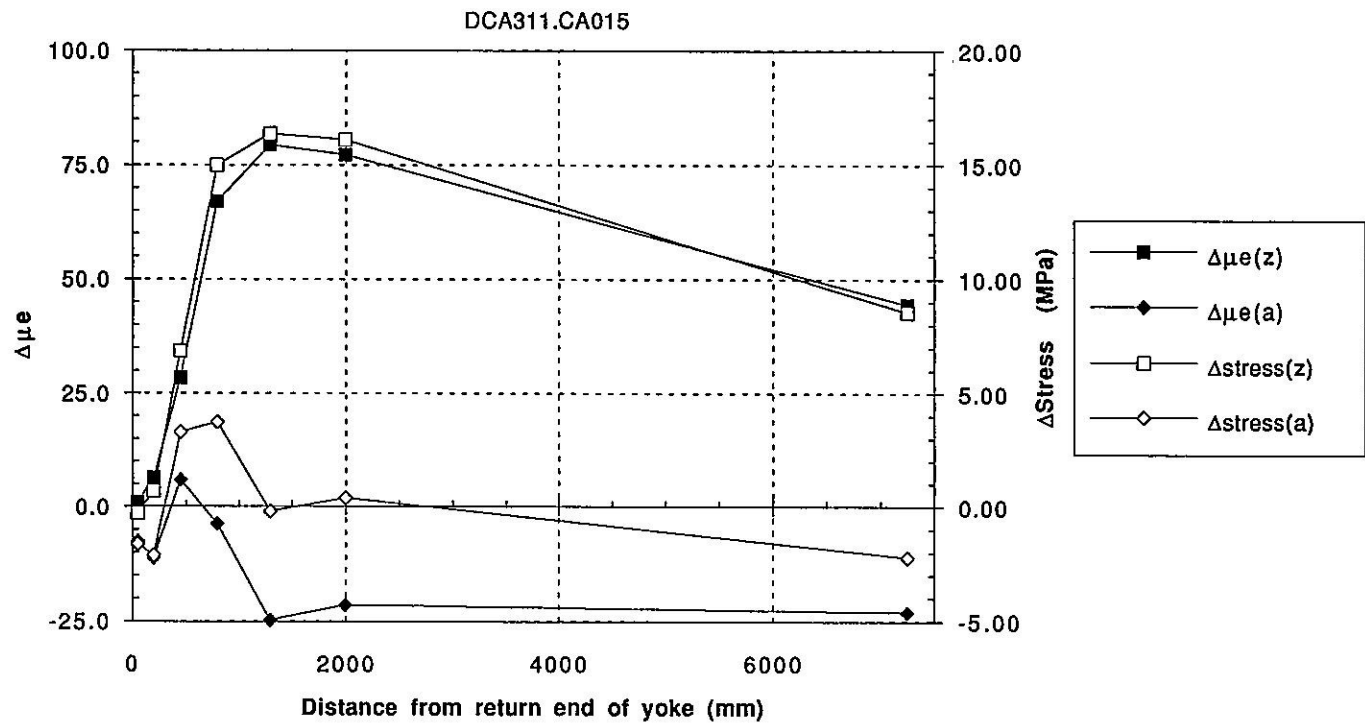


Figure 4

### DCA311 Shell Strain Gauges: Change to I=7660 A

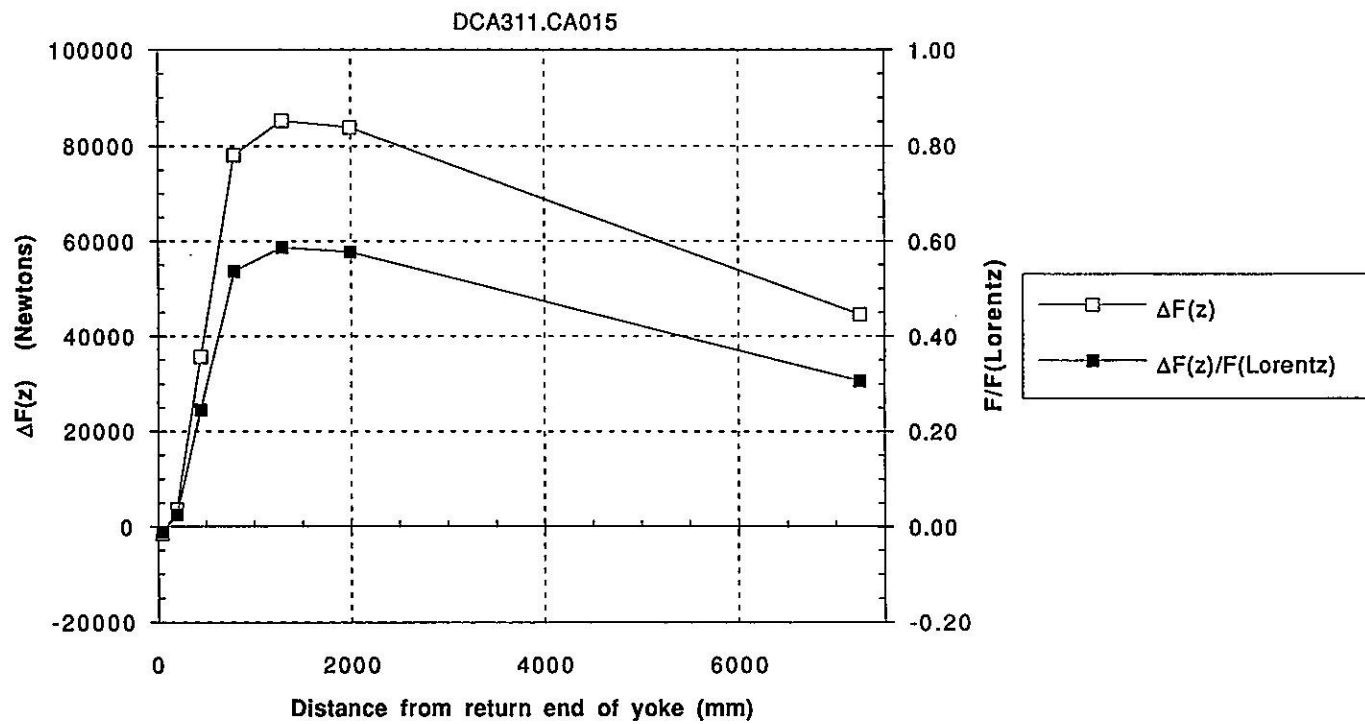


Figure 5

### Axial Shell Strain Change (DCA312.CA004)

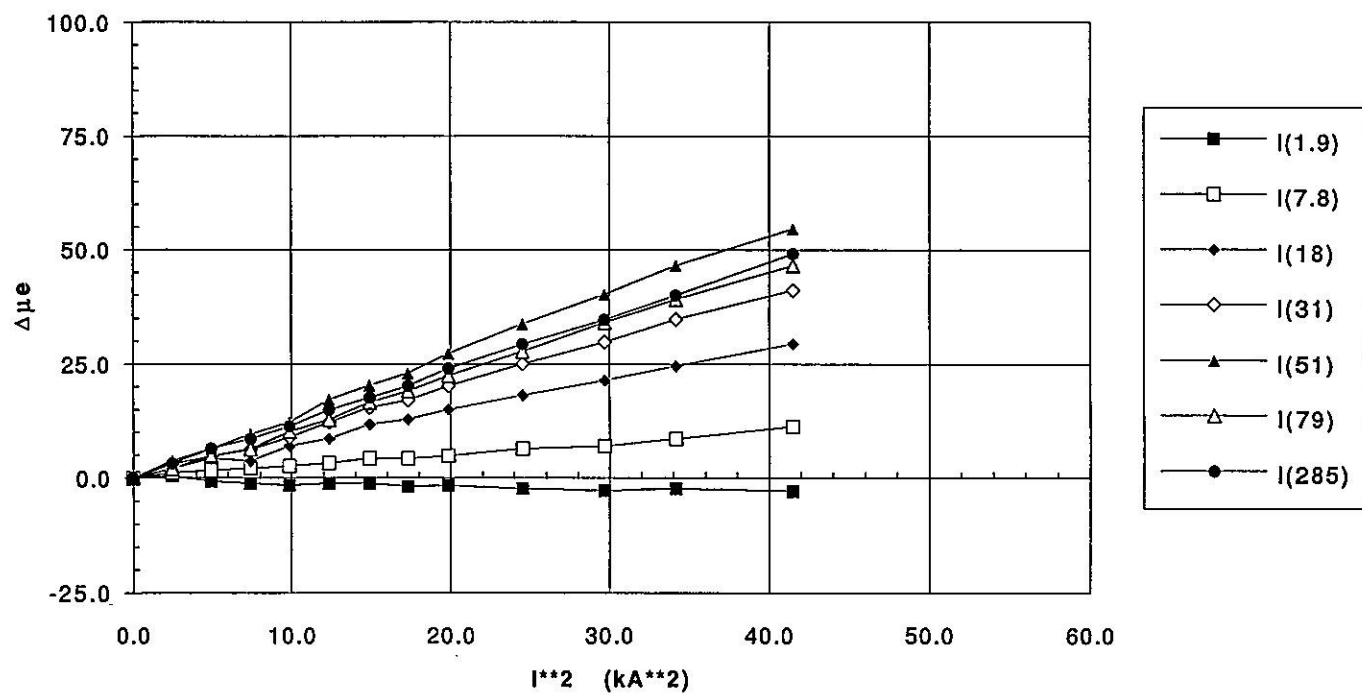


Figure 6

### Azimuthal Shell Strain Change (DCA312.CA004)

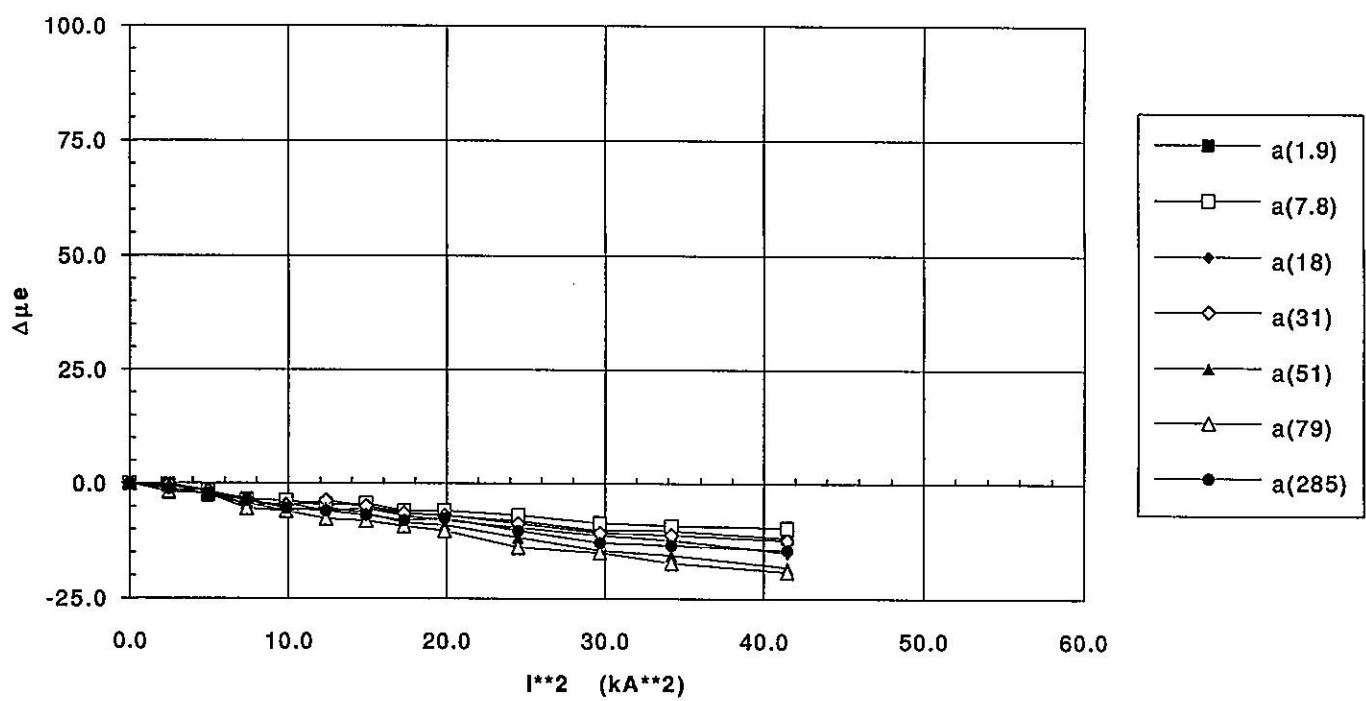


Figure 7

### DCA312 Shell Strain Gauges: Change to I=6440 A

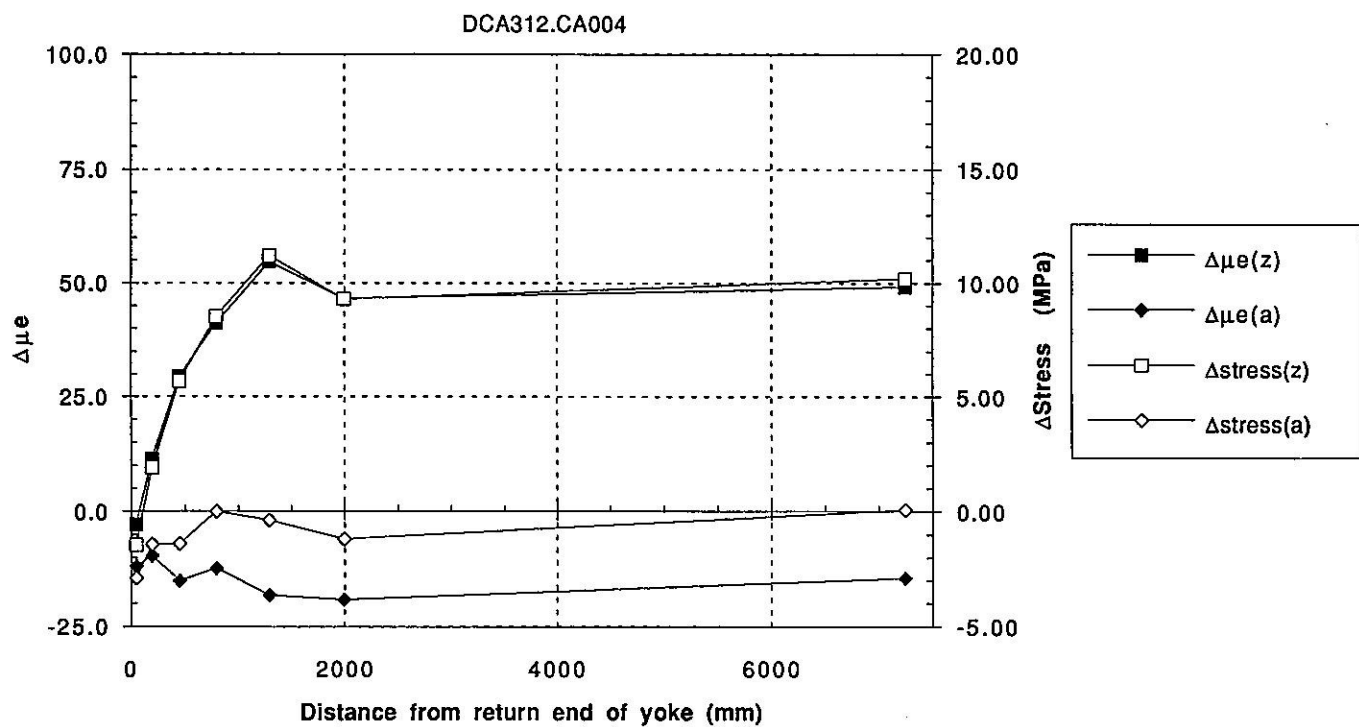


Figure 8

### DCA312 Shell Strain Gauges: Change to I=6440 A

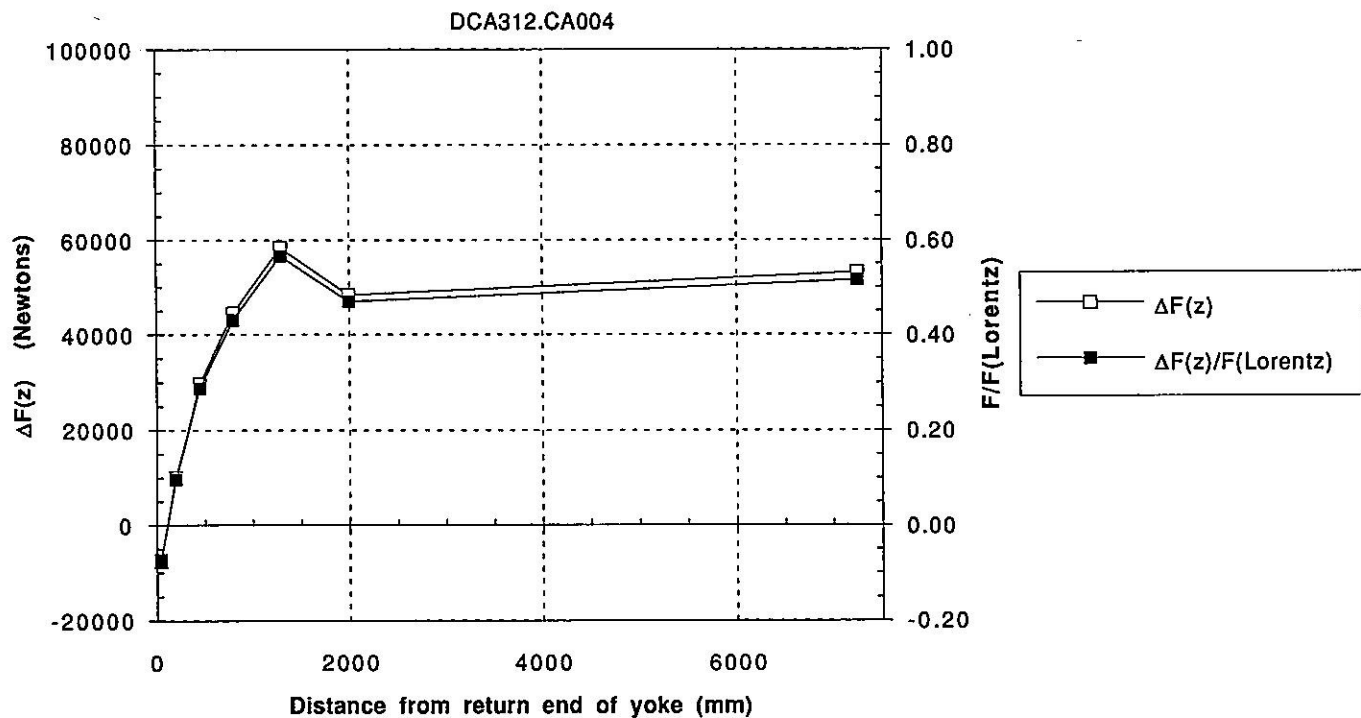


Figure 9